

Modeling of the Ground Motion for the Petropavlovsk Earthquake of November 24, 1971 ($M = 7.6$)

A. A. Gusev^{a,b}, E. M. Guseva^b, and V. M. Pavlov^b

^a *Institute of Volcanology and Seismology, Far East Division, Russian Academy of Sciences, bul'v. Piipa 9, Petropavlosk-Kamchatskii, 683006 Russia*

^b *Kamchatka Branch of the Geophysical Service of the Russian Academy of Sciences, Petropavlovsk-Kamchatskii, 683006 Russia*

Received September 9, 2008

Abstract—Based on the example of the strong earthquake of November 24, 1971, with the earthquake source near the Petropavlovsk-Kamchatskii, the new modeling technique of the strong ground motions within the broadband is tested. In this technique, the seismologically-substantiated models of the radiation source and elastic medium are used. The source is represented by an array of point radiation sources—dislocations with the random seismic moments (amplitudes) and with the random time functions. The new method of calculation of the Green functions is developed to describe the propagation of waves and residual displacements of a layered medium. The method is used for the simulation of the horizontal ground motion, recorded by a S5S-ISO instrument for the strong earthquake that took place on November 24, 1971 with the source near the Petropavlovsk-Kamchatskii (with a depth of 105 km). The position of the hypocenter, the sizes and the position of the fault, and “the source mechanism” were considered to be known a priori. By a trial and error method of the duration of the source process and only two spectral parameters, it was possible to simulate successfully the fundamental characteristics of the ground vibrations: the amplitude of acceleration, the velocity and displacement of the ground, their Fourier spectrum, the duration of the vibrations, and the spectrum of reaction. The surprisingly high level of high-frequency radiation, probably connected with the intraplate position of the source, is a specific feature of the source.

Keywords: earthquake source, accelerogram, modeling, and Kamchatka.

PACS numbers: 91.30.Ab

DOI: 10.1134/S1069351309050036

INTRODUCTION

In spite of the long-term investigations, the realistic simulation modeling of the strong ground motions in the case of an earthquake remains a difficult task. In the present work, the principles and an example of testing the new technique are described, which presents a decisive step in this direction. This technique is focused on the solution of a limited task: the modeling of the motion of rock ground from the earthquake's source of large magnitude within the broadband in the framework of the model of a layered and weakly inelastic medium. In a number of engineering and seismological situations, these restraints are unessential.

While the description of the propagation of an elastic disturbance from the source is, in principle, a straightforward problem of mathematical physics, the description of a radiation source causes a number of difficult questions. In a number of works, starting with the classical papers of Kostrov, a source is considered as a dynamic, spontaneously propagated crack in an elastic medium. However, this conceptually very attractive approach encountered a number of difficulties. Thus far, the observed localization

of the sliding process in the narrow running strip could not be simply explained. The other problem is the impossibility of predicting the observed behavior of the source spectra at high frequencies. At the same time precisely this part of the spectrum is of interest first of all for engineers.

For the problems of engineering seismology, the semi-empirical description of the radiation source, when theoretical considerations are combined with the generalization of observations, is an efficient alternative. The first step in this direction was the description of the family of focus spectra for sources of different magnitudes, first under the assumption of similarity [Haskell, 1966; Aki, 1967; Brune 1970] and, then, taking into account its violation [Gusev, 1983, 1984; Papageorgiou and Aki, 1985]. The next important step is the utilization of multielement source models. The model of the source of a large earthquake as a set of small isolated cracks or dislocations of the same type [Papageorgiou and Aki, 1983] or of different types [Blandford, 1975; Koyama, 1985], is the most developed one; but the model of a unique fault with sub-sources of the type of strong spots (“asperity”) was also proposed [Gusev, 1988, 1989]. With the help of the models of sub-sources—cracks it was possible to describe rather

well a set of data on strong motions. Nevertheless, it is necessary to note that these models are unsatisfactory tectonophysically: the long-term sliding across the fault is actually excluded in them, which contradicts the facts of seismic geology.

A good model should consider, on the one hand, the entire information obtained from the sources' inversions: the degree of sliding localization, the wave-numerical spectra of the final shear, etc. On the other hand, it should simulate successfully the high-frequency parameters, known from the analysis of accelerograms: the shape of the Fourier spectra, the amplitudes and statistics of the peaks of acceleration and velocity, and the duration of accelerograms. Thus far, only semi-empirical models make it possible to account for the factors enumerated. Further, exactly such a model is described. An ingenious variant of the stochastic model of the source with a set of point-like radiation sources with the appropriate time functions, arranged in the form of a lattice, is used. The time functions of individual radiation sources are combined with the appropriate Green functions, which describe the wave propagation in the medium; then, the results are summarized.

The parameters, which describe a particular source, can be divided into two basic groups: the physical parameters, which are fixed in a concrete calculation, and the "random parameters." The variation of the physical parameters makes it possible to consider the seismologically-specific character of the source, connected with variations in the natural factors (the relieved stress, the source depth, the velocity and the direction of fault propagation, etc.). The selection of the physical parameters is the necessary element for modeling the real ground motions. The "random parameters" are the initial values of random-number generators, whose variation determines a purely stochastic variability. The spread in values caused by these parameters determines the actually accessible quality of the fitting.

For testing the simulation system, in the present work, the modeling of the ground motion—recorded for the strong (of magnitude $M_w = 7.6$) intermediate (with a depth of 105 km for the hypocenter) earthquake of November 24, 1971 near the Petropavlovsk-Kamchatskii, with the earthquake's intensity at the point of recording ranging from five to six—is conducted.

MODELING TECHNIQUE

Source Modeling

The basis of the source–fault model is a classical model [Haskell, 1964, 1966], in which the source is represented as a rectangular shear dislocation, which appears via the one-sided propagation of the rectilinear fault front along the long side of the rectangle. At each point of the area the random process of the mutual sliding of the fault edges begins at the moment of arrival of the crack propagation front at this point and continues during a particular time interval, the "rise time". This

model is further generalized in the following way. The final shear, instead of the constant one, is a random function of two variables with the assigned 2D wave number power spectrum. The front of the fault propagation is not rectilinear, but circular, the point at the beginning of the fault propagation (i.e., the point of the crack–dislocation nucleation) is arbitrary, but the velocity of propagation of the fault front is a random function, which can be represented as a function of time or the distance passed by the front. The most important properties of the model accepted are the following:

- the source is represented as the lattice of point subsources–dislocations with an identical orientation of the sliding vectors and the normal vector;

- each subsource is turned on at the moment of the arrival of the front of the fault propagation at the corresponding subsource;

- the time functions of the subsources are random, non-Gaussian, and they are not mutually correlated;

- the seismic moment M_{0i} of each subsource is determined by the distribution function of the final jump of the displacement through the source area mentioned above.

The time functions of the subsources $\dot{M}_{0i}(t)$ are always non-negative and are modeled with the help of the Monte-Carlo method taking into account their assigned duration and assigned integral (equal to M_{0i}). The number of model subsources in principle is arbitrary, and for the case of a receiver near the source, can reach many hundreds. The model subsources themselves do not have a meaningful tectonophysical sense and serve only as an instrument of the source's numerical description.

In the modeling technique, the usually occurring non-Gaussian nature of the main distribution functions is taken into account, namely, for the values of the seismic moments of the subsources and for the amplitudes of the time function of each separate subsource. The logarithmically-normal law was accepted for these values. The spectrum of the random function of the final shear and the spectrum of the envelope of the time function of the subsource are accepted to be powerlike. As is known, a Gaussian random function with the power-law spectrum after exponentiation is transformed into a positive function, namely, the logarithmically-normal multifractal [Schmitt and Marsan, 2001]. In our case, both the distribution of the seismic moment, and the time function of the subsource relate to this class.

The spectra of subsources are selected on the basis of the requirement that the amplitude radiation spectrum of the subsource is close to the given ("target") spectrum. The "target" spectrum is assigned on the basis of the scaling law, taking into account, the seismic moment M_0 and the other parameters. In accordance with the empirical observations, the similarity of spectra in the narrow sense is not assumed.

The Calculation of the Medium's Response

For the calculation of the contribution of each sub-source to the ground motion in the receiver the new, effective calculation procedure of synthetic seismograms was used [Pavlov, 2002, 2006]. The procedure enables one to synthesize seismograms (the Green functions) from the point of the power dipole with the symmetrical tensor of the seismic moment, placed in the layered elastic half-space. Following the work of [Alekseev and Mikhailenko, 1978], the solution is represented in the form of series of horizontal functions with discrete values of the wave number, the roots of the Bessel functions. In order to determine the coefficients of the series ("the vertical functions"), ordinary differential equations are solved along the depth z (one equation for SH and two coupled equations for P–SV). The equations are solved analytically with the help of the introduction of impedances. For the SH waves the impedance is a scalar function z , which, on multiplication with the coefficient of the series for the displacement vector gives the corresponding coefficient of the series for the stress vector. For the P–SV waves, the impedance is the matrix function z and is determined analogously. First, the impedance is calculated; then, the unknown vertical functions are calculated with the help of the impedance. The calculations are carried out through the use of analytical formulas, which do not contain exponents, whose modulus exceeds the unit that provides numerical stability. The method applied provides an accurate wideband representation of the displacements from static to high-frequency terms.

The weak absorption in the media can be taken into account by the introduction of imaginary additives to the velocities of the elastic waves. However, in this way it is difficult to account for the dependence of the losses on the frequency. Since this factor is essential in the case of wideband (0–20 Hz) modeling, in the present work, a more primitive approach is used. The losses were considered to be dependent only on the hypocentral distance r , and it was considered that the losses for the amplitude spectrum take the form:

$$A(f)/A_0(f) = \exp(-\pi f(\kappa + r/c_s Q_s(f))), \quad (1)$$

where κ_0 is the parameter of the fixed losses beneath the station, r is the beam length, and c_s and Q_s are the mean values of the velocity and Q-factor along the beam for the S-waves. In this case, in the low-frequency part of the spectrum, where the absorption is small, inaccuracies in its estimation are, in general, insignificant. The absorption of the group of P-waves with this method of calculation is artificially overestimated, but the influence of this inaccuracy on the results is small because of the smallness of the relative amplitudes of the P-waves.

In order to obtain each component of the ground motion in the receiver, first, for each sub-source, the convolution of its time function with the appropriate Green function (which gives the contribution of this sub-source to the motion in the receiver) is carried out;

then, the contributions from all sub-sources are summarized.

The Modeling Program. The List of the Parameters of the Source and the Medium

The described algorithms are realized in the form of a modeling system: the AKSSIN program package. Its basic version is described in [Gusev and Pavlov, 2006]. Here, we present the list of the basic source and media parameters, which are the input parameters for the modeling system.

1. The coordinates and the depth of the center of the rectangular fault–source ("the macroseismic hypocenter"), its length L , its width W , and the moment of the magnitude M_w .
2. The angles of the bedding, the slope, and the sliding of the source area ("the source mechanism").
3. The number of sub-sources along the length n_L and along the width n_W (all in all $n_L n_W$ sub-sources).
4. The position of the starting point (the hypocenter) along L and W .
5. The parameters of the random dimensionless rock burst velocity: the mean is $Mach$, with a semirange DV of instantaneous values. The mean velocity is equal to $v_m = Mach \cdot c_s$.
6. The dimensionless rise time of C_H as a fraction of the time of propagation of the rock burst T_{pr} ($T_{rise} = C_H T_{pr}$). It was assumed that T_{rise} is the duration of the major part of the sliding process and its total time is equal to approximately $2T_{rise}$.
7. The parameters CV_l and CV_{xy} determine the degree of the non-Gaussian nature of the logarithmically-normal laws mentioned above for the functions of the sub-sources and for the function of the final shearing.
8. Exponent s in the power law for the isotropic 2D amplitude spectrum of the final shearing of form $S(k_x, k_y) \sim (k_x^2 + k_y^2)^{-s/2}$.
9. The initial values of the random number generator: for the final shearing, for the time functions of sub-sources, and for the instantaneous velocities of fault propagation.
10. The particular law of scaling of the source spectra $\dot{M}_0(f|M_w)$, tabulated or in the form of a formula; and the set of parameters for the fixation of a concrete spectrum.
11. The parameters of the layered medium and receivers: the coordinates and the values of κ_0 for the receivers and the vertical profile of the velocities and density, $Q_s(f)$.

THE INITIAL DATA FOR MODELING THE PETROPAVLOVSK EARTHQUAKE

The Petropavlovsk earthquake of November 24, 1971 [Gusev et al., 1975] (Fig. 1, Table 1), with a mag-

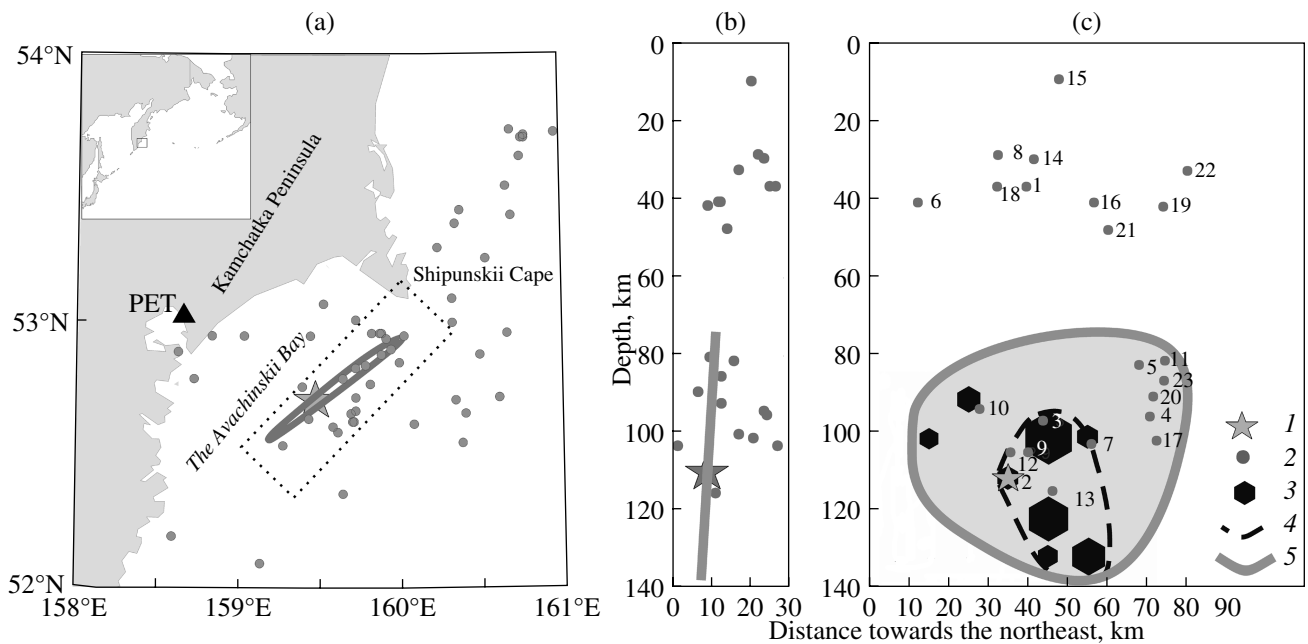


Fig. 1. Study area and geometry of the source area: (a) map-diagram, (b) and (c) sections within the limits of the dashed rectangle in (a) along its narrow and wide sides. Designations: (1) the hypocenter of the main shock, (2) the hypocenters of the foreshock (number 1, advance 24 min) and aftershocks during the first two months according to the regional catalog; (3) subcenters (the source process components [Fukao and Kikuchi, 1987]); (4) the source region after 15 s according to [Fukao and Kikuchi, 1987]; (5) the source area, accepted in this work. The triangle designates the seismic station “Petropavlovsk” in Petropavlovsk-Kamchatskii. The position of the study area is presented in the inset.

nitude of $M_s = 7.2$, had an intensity in Petropavlovsk-Kamchatskii (located at a distance of approximately 125 km from the hypocenter) ranging from seven on the average ground to five–six at the recording point. The epicenters of the weak foreshocks and aftershocks, according to the catalog of the local seismic network

(<http://www.emsd.iks.ru>) are presented in Fig. 1. The region of the epicenters specifies the strike azimuth of the source: approximately 45°NE, at a small angle to the orientation of the structures of the Kurile-Kamchatka zone (30°–35°). The localization of the subcenters—the stages of the fault’s development in the

Table 1. Published source parameters

No.	ϕ, λ°	$h, \text{ km}$	$L, \text{ km}$	$W, \text{ km}$	$d, \text{ s}$	$v_r, \text{ km/s}$	ϕ_s	δ_s	λ_s	M_w	Reference
1	52.7 159.6	100 (d)	70 ⁽¹⁾	—	—	—	60	80	85	—	[Gusev et al., 1975]
2	52.77 159.66	100 (d)	30 ⁽²⁾	30 ⁽²⁾	6–8 ⁽³⁾	1.2, 4.3 ⁽⁴⁾	40	88	110	7.3–7.5P, 7.7R	[Zobin, 1984; Zobin et al., 1988]
3	52.9 152.2	112 (d) 95–130 (r)	35–40 ⁽⁵⁾	45	14, 50 ⁽⁵⁾	1.1	43	83	90	7.2P	[Fukao and Kikuchi, 1987]
4	52.77 159.66(c)	95 (c)	—	—	12	—	165 ⁽⁶⁾	10 ⁽⁶⁾	40 ⁽⁶⁾	7.1P	[Gorbatov et al., 1997]
5	52.71 159.47 52.79 159.59(c)	105 (d) 75–135 (r)	70 (40(NE), 30(SW))	60	45	1.1	43	83	120	7.65	Present work

ϕ, λ are the latitude and longitude of the epicenter and the center of the source area (marked by “c”), h is the depth of the instrumental hypocenter (“d”), the center of gravity or “centroid” (“c”) or the range of the depths of the extended source (“d”); L is the horizontal extension of the source and the length of its arms towards the northeast (NE) and southwest (SW) from the epicenter; W is the vertical extension of the source, in this case, almost coinciding with its width; d is the duration of the source process or its stages; v_r is the velocity of the fault propagation; ϕ_s, δ_s , and λ_s are the strike azimuth and the impact angle of the accepted fault plane and the corresponding slide angle; M_w is the moment magnitude for the P -waves (P) or Rayleigh waves (R). Notes: (1) extension of the chain of aftershocks, (2) our lower-bound estimate from the distance between the well-expressed subcenters, (3) the relative time delay between the subcenters, (4) variants of the velocity estimates on this basis, (5) the values of the size and duration for the initial stage and for the process as a whole, (6) all other authors considered this (gently sloping) nodal plane to be auxiliary.

source, according to the inversion of teleseismic P -waves, carried out in the detailed work [Fukao and Kikuchi, 1987]—is also plotted in Fig. 1. The probable boundary of the source area is plotted according to the reference data. The degree of reliability of the drawn boundary is limited. First, the lower part of the source area, plotted only according to the results presented in [Fukao and Kikuchi, 1987], penetrates by 15–20 km into the aseismic layer of the ocean platform. Second, foreshock (No. 1) and a number of aftershocks arose at depths of $H = 20$ –40 km above the assumed source and our conclusion that the source did not penetrate at these depths is just a hypothesis. We proceeded from the known tendency, that only the sources of intermediate depths (in contrast to the shallow-focus) form a small number of aftershocks. Therefore, the small number of weak aftershocks in the upper group ($H = 20$ –40 km) contradicts the idea about the penetration at this level of the fault–source: in that case, a larger (by hundreds of times) number of aftershocks should be expected. More probably this group has the nature of the induced activation of weak seismicity near, but not inside, the source. (Later, in March–August 1972, in the same zone a weak swarm of earthquakes occurred, which, possibly, outlined the zone of the aseismic sliding, provoked by the source of 1971.)

Now, we shall discuss the source geometry and kinematics on the basis of the previous works (see Table 1). According to [Fukao and Kikuchi, 1987], first, the source developed “fan-shaped”: it was asymmetric in plan view, towards the northeast, and simultaneously approximately symmetrical upward and downward. This phase of the source’s development lasted up to 12–15 s [Gorbatov et al., 1997; Fukao and Kikuchi, 1987], and enveloped a distance of approximately 30 km in plan view and 20–40 km along the vertical axis. Further development is observed with a great degree of uncertainty. Judging by the position of the aftershocks, the final fault has an approximately isometric shape, with the geometric center near the hypocenter. The final size of the source in plan view is approximately 70 km and along the vertical axis is approximately 60 km. The total duration of the source process according to [Fukao and Kikuchi, 1987] is up to 50 s. The propagation velocity of the source according to [Fukao and Kikuchi, 1987] and Fig. 1 is about 1.0–1.1 km/s. This is a low value: the Mach number $Mach = v_r/c_s$, amounts to only 0.23–0.25, against the typical value of 0.6–0.8.

The source mechanism was accepted according to [Fukao and Kikuchi, 1987]: the near-vertical reverse fault with the rising of the southeastern wing. The initial value of the sliding angle (90°) contradicted the picture of record and the accepted value of 110° was found by selection (see below). For the value of the moment’s magnitude, there are also values within a sufficiently wide interval. According to the data for P -waves, estimates of M_w within the range of 7.1–7.5 were obtained. The low estimates correspond to accounting for only the first 15 s of the motion, so there are no significant

Table 2. Accepted velocity section for the PET station

h_{top} , km	ρ , g/cm ³	c_p , km/s	c_s , km/s
0.0	2.3	1.7	0.95
0.025	2.5	2.7	1.5
0.5	2.5	4	2.22
5	2.7	5.8	3.35
20	2.7	6.7	3.87
35	3.3	7.8	4.5
120	3.3	8.1	4.74

contradictions here. For the Rayleigh waves there are estimates of up to $M_w = 7.7$. The modeling was started by assigning $M_w = 7.5$; but $M_w = 7.65$ was accepted as the final value (see below).

Now, we will describe the source model accepted in our calculations. The fault is the rectangle with a size of 70×60 km, covering a smooth contour (Fig. 1c). The hypocenter, the mean velocity of fault propagation, the source mechanism, and the seismic moment are given in Table 1. A number of source parameters were also rigidly assigned, namely: $DV = 0.75$, $C_H = 0.1$, $L = 70$ km, $W = 60$ km, $CV_t = 0.7$, $CV_{xy} = 0.85$, and $s = 12$. In this case, the experience of the successful simultaneous simulation of the records of 19 stations near the source, carried out in [Gusev and Pavlov, 2006], was taken into account. The velocity section of the medium (Table 2) is accepted according to the usual Kamchatka model of Kuzin, but the tops of the section are described in more details. The attenuation model is accepted in the form $Q_S(f) = 195 f^{0.4}$ with $f > 1$ Hz, $Q_S(f) = \text{const} = 195$ with $f < 1$ Hz, and $\kappa_{0S} = 0.015$ s. This model is chosen on the basis of the previously studied properties of attenuation near Petropavlovsk-Kamchatskii [Gusev and Shumilina, 1999; Abubakirov, 2005]. The model was refined according to the records of close earthquakes with $S-P < 3$ s and, simultaneously, the estimate of κ_{0S} was obtained.

The results of variance model calculations were compared with the record of the Petropavlovsk earthquake at the Petropavlovsk-Kamchatskii seismic station (PET) [Shteinberg et al., 1975]; the description of instrumentation is also presented there. The ground conditions are the intrusion of gabbro-diabases. Two horizontal components of motion were recorded on the photographic film by a S5S-ISO velocigraf. The quality of this unique record was far from ideal. In particular, a significant problem was the nonuniformity of the film’s transport in the oscillograph in the presence of ground fluctuations and the mounting system of the oscillograph. This defect is essentially corrected by the application (on digitizing) of the linear interpolation of time moments within the limits of each interval between the oscillogram’s time marks on the film (the algorithm is implemented by A.G. Petukhin within the framework of methodology presented in [Gusev et al., 2006]).

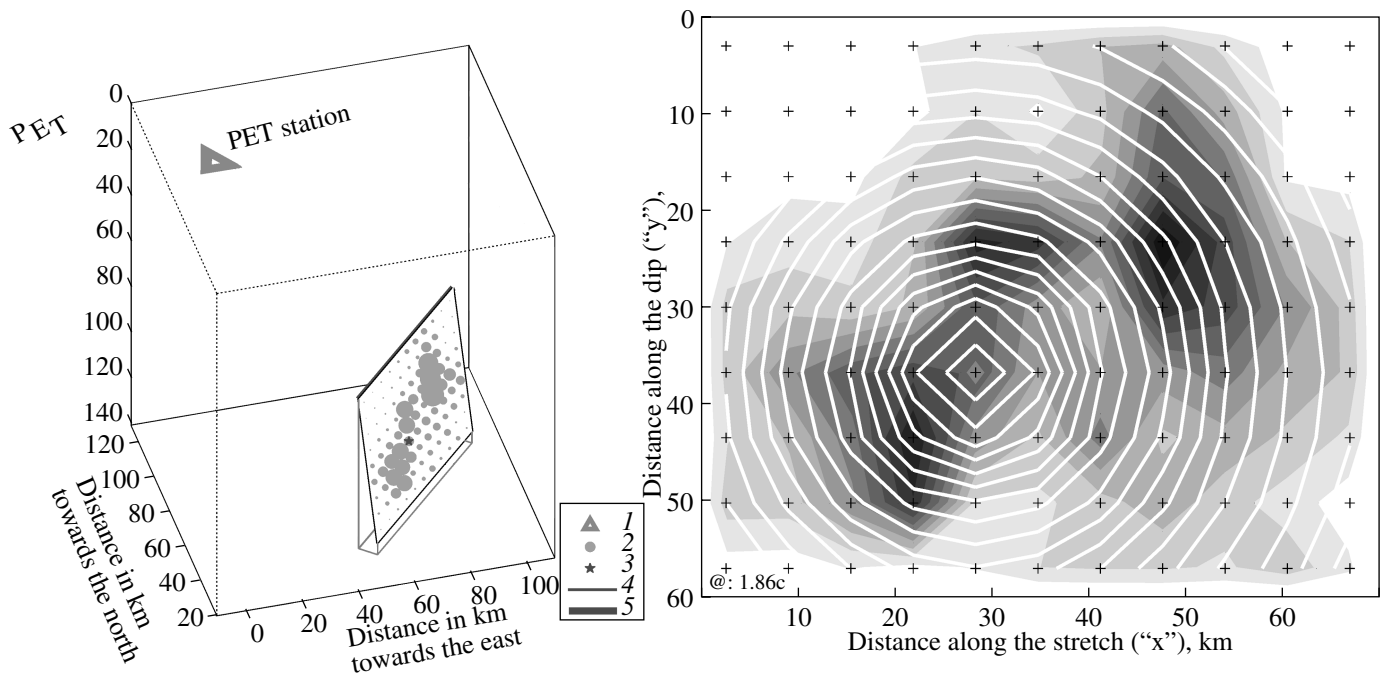


Fig. 2. Perspective view of (a) the position of the model source and PET station and (b) the details of the distribution of subsources and front kinematics in this source. Designations to the case (a): (1) seismic station, (2) subsurface, (3) starting point (the hypocenter), (4), (5) the edges of the rectangle-source, (5) the upper edge. The grid of subsources 11×9 is accepted, their “amplitudes” (the value of the final shear) are depicted by the value of the circle on (a) in the form of the gray levels on (b). The white outlines on (b) designate the position of the front of the model fault every 1.9 s. Deviations and shapes of fronts from the circles (the artefact of the interpolation program of the fronts between the point sources).

Finally, a relatively reliable recording of the frequency band from 0.05–0.07 to 15–25 Hz is provided.

SELECTION OF THE SOURCE PARAMETERS AND THE RESULTS OF MODELING

The results of the modeling of the ground vibrations caused by the earthquake of November 24, 1971 with the use of the AKSSIN program package are given below. The methodology was tested via the comparison of the model’s ground motions and the real records of the earthquake. For the best understanding of the modeling procedure we will somewhat disturb the logical sequence of the paper: first, we will illustrate the methodology with the use of the plots for the final version of model, with the parameters already selected, and we will discuss the selection procedure of the parameters later.

Results of the Modeling

The problem’s geometry and the 2D distribution of the final slip are given in Fig. 2. To illustrate the methodology, the grid of the subsources was selected to be sufficiently detailed: 11×9 . (For a station at a distance, which exceeds the source size, even more coarse mesh would be sufficient, for example, 9×3). In Fig. 2b, attention should be focused on the nonuniform velocity

of the fault propagation. This factor, as the numerical experiments show, makes a significant contribution to the variability of the resulting motion.

The time functions of each subsurface are given in Fig. 3. The duration of each of them (about 8 s) is close to $2T_{\text{rise}}$. Along the vertical axis of the figure, one can see nine groups of traces for each depth level. There are eleven traces in each group. For greater clarity, the magnified trace for the earliest subsurface (in the hypocenter) is presented; qualitatively, it does not differ from the remaining 98 traces. At the bottom of Fig. 3, the source time function is given: the first derivative $\dot{M}_0(t)$ of the function of seismic moment of the point dipole source, which is equivalent to the earthquake source. The shape of this curve is identical to the shape of the signal of displacement of the transverse or longitudinal waves, which would be obtained in a homogeneous medium in the far-field zone of the source by the receiver, located on the normal to the source area. This function is simply the sum of the corresponding functions of subsources. In Figs. 4 and 5, the model and actual signals of displacement, velocities and accelerations and, also, the corresponding smoothed Fourier spectra are compared.

Considering Figs. 3, 4, and 5, one should take into account the following circumstance. First, the given illustrations reflect one among many models of the

same type, generated for different initial values of the random number generator and with fixed values of the source's physical parameters. The structure of the scatter between the implementations was studied in detail in [Gusev and Pavlov, 2006]. According to these estimates, the scatter with the maximum amplitudes, due to this factor, should amount to approximately 15–25%. Secondly, it is necessary to keep in mind that the used calculation model is aimed only on the reasonable simulation of amplitudes, durations, and spectral properties of real vibrations. This problem, in our opinion, is successfully solved. However, the problem of the reproduction by the model of the actual ground motion in details, i.e., “the inverse problem for the source,” was not posed and was not solved.

Adjustment of the Source Parameters and Spectrum Modeling

Now, we will describe the process of adjusting the parameters, which was conducted via the trial-and-error method. The following parameters were adjusted: the angle of slide λ_s , the moment magnitude M_w , the parameter *Mach*, and also two parameters, which describe the spectrum's shape. Regarding λ_s and M_w , first, we attempted to fix them according to independent data: $\lambda_s = 90^\circ$ ([Fukao and Kikuchi, 1987]) and $M_w = 7.5$ (a compromise among many sources). However, it turned out that this adjustment was clearly unsuccessful. The actual ratio of the observed amplitudes of displacement and velocity on the NS and EW components clearly excludes the initial value of λ_s ; the accepted value of $\lambda_s = 110^\circ$ is obtained sufficiently reliably (the uncertainty is approximately 5°) and it barely contradicts the signs of teleseismic *P*-waves. With respect to M_w , it turned out that the initial value accepted is too low and can provide the observed level of the amplitudes of displacement only with the very exotic shapes of spectra. The accepted value of $M_w = 7.65$ is, in essence, the minimum reasonable estimate. However, the value of $M_w = 7.65$ is already at the upper limit of acceptability from the point of view of the agreement of our results with the teleseismic estimates of M_w ; therefore, further, it was fixed. The accepted value of the parameter *Mach* = 0.24 was adjusted to obtain the velocigram duration, which is close to the observed one. In our case, this duration is defined by the duration of the source process, which, in turn, with the fixed *L*, *W*, and hypocenter, is defined exactly by the value of *Mach*. It should be noted that *Mach* = 0.24 is in unexpectedly strong agreement with the estimate from [Fukao and Kikuchi, 1987], carried out through teleseismic surveying.

The adjustment of spectra was conducted in the following way. First, the variants of the source spectrum according to the Brune “ ω^2 ” model [Brune, 1970] and from the family [Gusev, 1983] were checked. In both these models, the source spectrum is assigned by the values of M_w and relieved stress $\Delta\sigma$ (the two-parameter

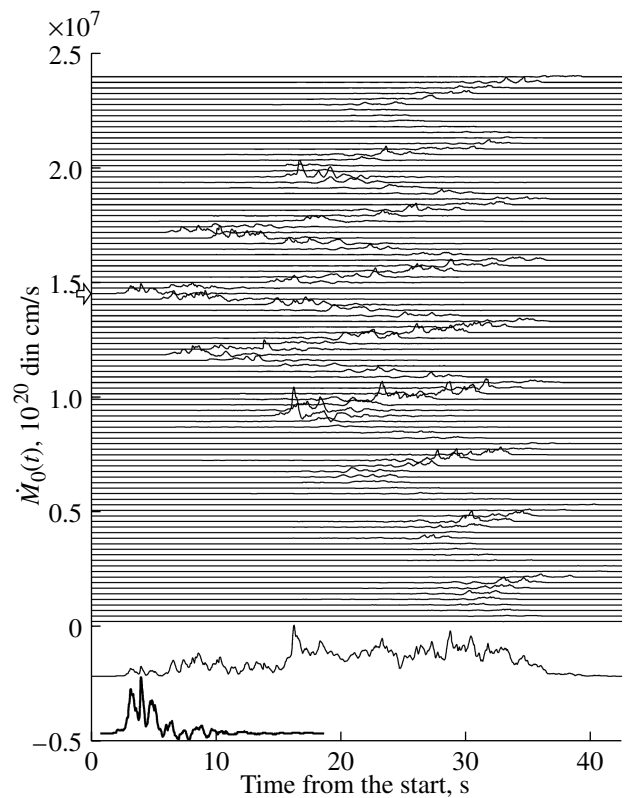


Fig. 3. Variant of source time functions ($\dot{M}_0(t)$ or “displacement”) for 99 subsources. The following are separately presented at the bottom: the time function of the summarized source and, repeatedly with an increased scale, the time function of the subsurface in the hypocenter (its initial form is marked by the pointer).

model: $\dot{M}_0(f|M_w, \Delta\sigma)$). In this case, for the spectra from [Gusev, 1983] the account of $\Delta\sigma$ is carried out by the modification of the initial tables (see [Gusev and Pavlov, 2006]). At the qualitative level it became immediately clear that the actual level of the source's spectrum of acceleration at the high $\ddot{M}_0(f)|_{f \gg f_c} = A_{HF}$ frequencies is unexpectedly high, and that the spectrum's shape is far from single-peaked, with the single corner-frequency “ ω^2 ” of the Brune model spectrum. The double-peaked spectra from the family [Gusev, 1983] give a somewhat better but, nevertheless, unacceptable description of the data. Therefore, we used a more complex and sufficiently more flexible multiparametric model of the double-peaked spectrum in the form of analytical formula according to [Atkinson, 1993] (the spectrum of “2Brune” type), of the form

$$\dot{M}_0(f) = M_0 \left[\frac{(1 - \epsilon)}{1 + (f/f_a)^2} + \frac{\epsilon}{1 + (f/f_b)^2} \right]. \quad (2)$$

Here, the parameter f_a corresponds to the usual corner-frequency f_c according to Brune. This formula has four

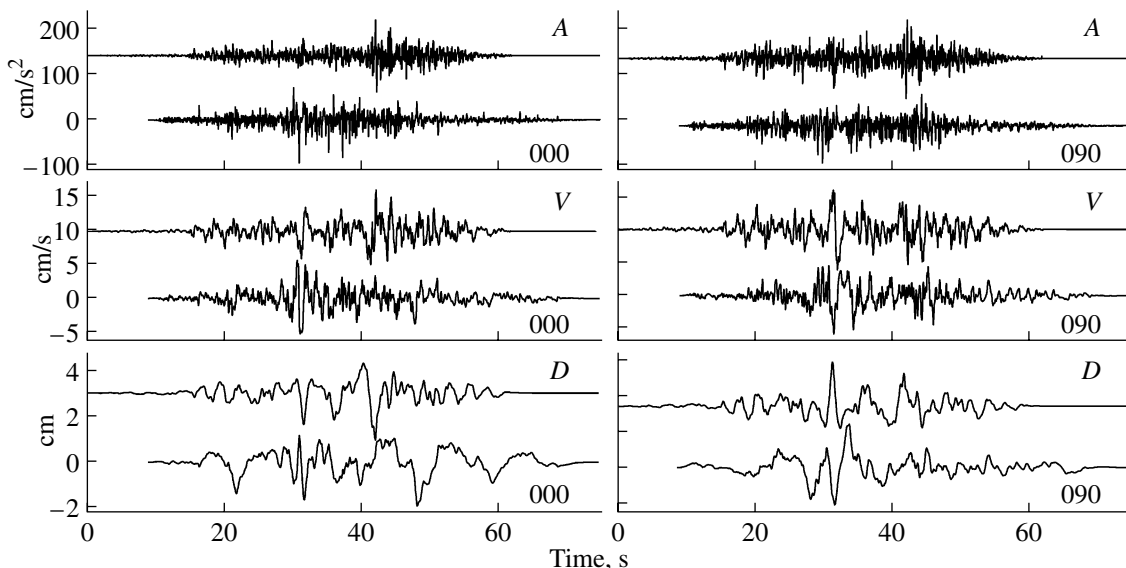


Fig. 4. Variant of time functions—the results of modeling of the ground motion (at the top of each framework) in comparison with the observed records (at the bottom of the framework) in a single scale. The high-frequency filter with the cutoff frequency at the level of -3 dB, equal to 0.07 Hz, was applied both to the actual and to the model signals. The relative shift of the beginning of the countdown of the real and model record is arbitrary. From top to bottom, three pairs of the plots of signals are presented: the acceleration, the velocity, and the displacement. The left-hand column in the pair is the NS component and the right-hand column is the EW component. The given traces of displacement have a somewhat conditional nature; their shape substantially depends on the selection of the cutoff frequency and even on the details of the high-frequency filter, applied to the observed and model data. The displacement reconstructed in the band up to $f = 0$ included the static component (the step) with the amplitude -2 cm for NS and $+3.5$ cm for EW.

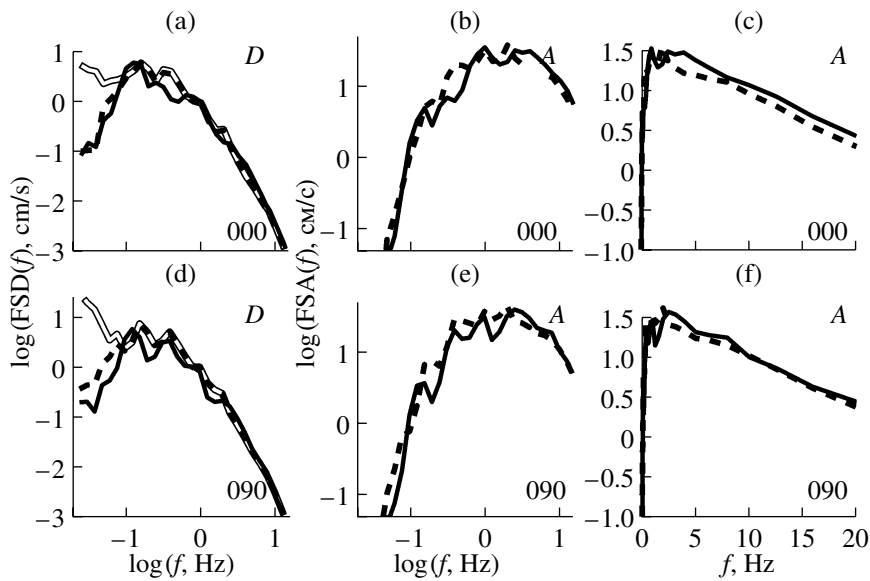


Fig. 5. Amplitude of the Fourier spectra of (a); (d) displacement; and (b), (c), (e), and (f) acceleration of the ground motion for the variant of model time functions presented in Fig. 4. The double line represents the model spectrum, the solid and dashed lines designate the observed and model spectra after the filtering. The pair (c) and (f) have a natural scale along the abscissa and the logarithms are plotted along the remaining scales. Components: (a), (b), (c) NS; (d), (e), and (f) EW.

parameters: M_0 ($\log M_0 = 1.5(M_w + 10.7)$), f_a, f_b , and ϵ . Instead of the latter of these, the clearer parameter A_{HF}

was used. In this case it was accepted that $\log A_{HF}$ is scaled with $\log M_0$ as $\log A_{HF} = (1/3)\log M_0 + \text{const}$ as in the

“ ω^2 ” model. The dimensionless parameter $C_{ba} = f_b/f_a$ was also introduced. Now, for the parameter ε we obtain:

$$\varepsilon = \left(\frac{1}{C_{ba}^2 - 1} \right) \left(\frac{A_{HF}}{(2\pi f_a)^2 M_0} - 1 \right). \quad (3)$$

The new set of four parameters is the following: M_0 , f_a , C_{ba} and A_{HF} .

In this model, it is accepted that in its high-frequency part the source's spectrum of acceleration is flat, in accordance with the hypothesis of the “ ω^2 ” model, but its level is not connected with the value of $\Delta\sigma$ [Izutani, 1984]. The adjustment of the parameter M_w is described above. The value of $f_a = f_c$ is found from M_w , in accordance with the mean trend of the corner-frequencies of the family of typical source spectra in Fig. 3 [Gusev, 1983]. There, this trend is represented in graphic form, and as a formula it can be written as follows:

$$\log f_c = -2.25 - 0.5 M_w = 7.6 - (1/3) \log M_0, \quad (4)$$

that gives for $M_w = 7.65$ ($\log M_0 = 27.525$) $f_c = 0.0266$ Hz. Generally speaking, this estimate of f_c from M_w is valid only with the typical mean value of $\Delta\sigma$ (about 40 bars for the set of spectra [Gusev, 1983]). In this case, this is a feasible approach to adjusting f_c , since the value of the source area $S = \pi LW/4$ is very close to the expected value determined by the formula $\log S = 0.5 M_w = 4.1$ from [Gusev and Melnikova, 1990], which can be accepted as the reference value. The values of the other two parameters were found by searching, with the adjusted values amounting to $C_{ba} = 21$ and $\log A_{HF} = 27.33$; in this case $f_b = 0.56$ Hz and $\varepsilon = 0.0496$. From the accepted corner-frequency $f_a = f_c = 0.0266$ Hz, it is possible to estimate the typical (for $M_w = 7.65$) source duration, which has to be equal to about $1/0.0266 = 38$ s. This is comparable with the actual number of 45 s. This agreement is the result of the mutual compensation for the effects of the low $Mach$, on the one hand, and the total effect of the isometric form and the double-sided fault propagation, on the other hand. In the more usual case of the elongated one-sided fault the agreement would disappear.

The degree of the numerical agreement of the observed and calculated maximum amplitudes of displacement, velocities, and accelerations is within the limits of 10–15%. We also estimated the agreement of the reaction of the observed and model spectra. Divergences for the averages for two components and on each of the four chosen frequency bands 0.07–0.3, 0.3–1.0, 1.0–3.0, and 3.0–12.0 Hz, are small, amounting to not more than 5%. For the individual frequencies there are outliers up to +60% / –35%, that under the conditions of the absence of systematic differences it is possible to consider as quite acceptable.

Thus, we succeeded in reasonably adjusting the shape and the level of the actual source spectrum by

applying the trial and error method to two parameters: A_{HF} and C_{ba} . Although the values of $Mach$ and M_w were also adjusted, they varied only within narrow limits; essentially, these values were fixed according to independent data. The approach applied to the data description appears to have been successful, since within its framework, by the adjustment of only two parameters, it was possible to simultaneously fit with the observations the levels of the amplitudes for the accelerations, the velocities, the displacements, and also the levels of the Fourier spectra and reaction spectra within the broadband of frequencies.

Results and Discussion

Now, we will compare our result with other data. First, it should be noted that the value of $\log A_{HF} = 27.33$ noticeably exceeds the Japanese average for the interplate source with $M_w = 7.65$, for which, according to the summary presented in [Irikura, 2006], one should expect $\log A_{HF}$ [din cm/s³] = $(1/3) \log M_0$ [din cm] + 17.39 = 26.56. We can designate the deviation from this trend as $\delta \log A_{HF}$; in our case $\delta \log A_{HF} = +0.77$. For the intraplate shocks in Japan, for the same source, $\delta \log A_{HF}$ amounts to approximately +0.5–0.6. The source of 1971 is unambiguously intraplate. This is clearly seen in Fig. 1b, where the arrangement of the upper group of hypocenters at depths of 20–45 km exactly corresponds to the position of the boundary of the plates on the section across the arc structures. Furthermore, the source of 1971 is a source of intermediate depth. This factor frequently leads to a noticeable increase of the level of high frequencies (see, for example, [Gusev and Melnikova, 1990]). These factors are independent and their contributions should be summarized. Thus, it is possible to consider that the value of A_{HF} evaluated by us is in reasonable agreement with the data concerning Japan.

Parameter f_b governs the position of the right-hand peak in the spectrum. For the data on Japan, the very fact of the double-peaked shape of the spectra was revealed repeatedly [Koyama et al., 1982; Izutani, 1984], but quantitatively this property has not been studied. The double-peaked nature of the California spectra has been studied better. With the same value of M_w , within the framework of the “2Brune” model, the formula from [Atkinson and Silva, 1997] gives (for the California conditions) $f_b = 0.29$ Hz, which indicates a specific, but not especially sharp, difference. On the whole, the obtained description of the spectrum does not contradict the results of well-studied seismoactive zones.

CONCLUSIONS

The new version of the methodology and software for the seismologically-substantiated modeling of

ground motions is successfully tested on the recorded data of the strong earthquake of November 24, 1971 in the region of Petropavlovsk-Kamchatskii. This is the strongest of the earthquakes recorded here; therefore, its modeling, in addition to being of great scientific interest, is also of great practical interest. For the first time for data on the Far East of Russia, it was possible within the broadband to simulate successfully the actual record of an earthquake and to estimate the parameters of its source. In this case, essentially, our ideas—on the structure of the medium near the Kamchatka Peninsula (the velocity and absorption), the general description of the spatio-temporal source structure, and the used variant of the parametrization of the double-peak source spectra—passed a complex test. By the adjustment of only two parameters it was possible to assign the probable source spectrum, on the basis of which the observations within the broadband were successfully described. As a result, the model values of amplitudes and levels of spectra, which are close to the observed values, were obtained.

ACKNOWLEDGMENTS

This work was supported by the Russian Foundation for Basic Research, project no. 07-05-00775.

REFERENCES

1. I. R. Abubakirov, "Evaluation of the Attenuation Characteristics of Transverse Waves in the Lithosphere of Kamchatka according to Observations of the "Petropavlovsk" Digital Broadband Station," *Fizika Zemli*, No. 10, 46–58 (2005).
2. E. Aki, "Scaling Law of Seismic Spectrum," *J. Geophys. Res.*, **72**, 1217–1231 (1967).
3. A. S. Alekseev and B. G. Mikhailenko, "The Method of Calculation of the Theoretical Seismograms for the Models of Complex Structure Media," *Dokl. Akad. Nauk USSR*, **240**(5), 1062–1065 (1978).
4. G. M. Atkinson, "Earthquake Source Spectra in Eastern North America," *Bull. Seismol. Soc. Am.* **83**, 1778–1798 (1993).
5. G. M. Atkinson and W. Silva, "An Empirical Study of Earthquake Source Spectra for California Earthquakes," *Bull. Seismol. Soc. Am.* **87**, 97–113 (1997).
6. A. A. Blandford, "A Source Model for Complex Earthquakes," *Bull. Seismol. Soc. Am.* **65**, 1385–1405 (1975).
7. J. N. Brune, "Tectonic Stress and the Spectra of Seismic Shear Waves from Earthquakes," *J. Geophys. Res.* **75**, 4997–5009 (1970).
8. Y. Fukao and M. Kikuchi, "Source Retrieval for Mantle Earthquakes by Iterative Deconvolution of Long-Period P-Waves," *Tectonophysics* **144**, 249–269 (1987).
9. A. Gorbatov, V. Kostoglodov, G. Suarez, and E. Gordeev, "Seismicity and Structure of the Kamchatka Subduction Zone," *J. Geophys. Res.* **102**, 17883–17898 (1997).
10. A. A. Gusev, "Descriptive Statistical Model of Earthquake Source Radiation and its Application to an Estimation of Short-Period Strong Motion," *Geophys. J. Roy. Astr. Soc.* **74**, 787–808 (1983).
11. A. A. Gusev, "Descriptive Statistical Model of the Earthquake Source Radiation and its Application to Estimation of Short-Term Strong Motion," *Vulkanologiya i Seismologiya*, No. 1, 3–22 (1984).
12. A. A. Gusev, "Multiasperity Fault Model and the Nature of Short-Period Subsources," *Pure Appl. Geophys.* **130**, 635–660 (1989).
13. A. A. Gusev, "The Model of Earthquake Source with Multiple Asperity," *Vulkanologiya i Seismologiya*, No. 1, 41–55 (1988).
14. A. A. Gusev and V. N. Melnikova, "Relations between Magnitudes: the Worldwide and for Kamchatka," *Vulkanologiya i Seismologiya*, No. 6, 55–63 (1990).
15. A. A. Gusev and V. M. Pavlov, "Wideband Simulation of Earthquake Ground Motion by a Spectrum-Matching, Multiple-Pulse Technique," *1st Europ. Conf. Earthq. Eng. Seismol.* (Proceedings CD, Paper 408, Geneva, 2006) pp. 1–10.
16. A. A. Gusev, A. G. Petukhin, E. M. Gusev et al., "Mean Fourier Spectra of Strong Ground Motion during Kamchatka Earthquakes," *Vulkanologiya i Seismologiya*, No. 5, 60–70 (2006).
17. A. A. Gusev and L. S. Shumilina, "The Modeling of Intensity–Magnitude–Distance Coupling in terms of the Incoherent Extended Source Model," *Vulkanologiya i Seismologiya*, No. 4–5, 29–40 (1999).
18. A. A. Gusev, V. M. Zobin, A. M. Kondratenko, and L. S. Shumilina, "Petropavlovsk Earthquake of November 24 (25), 1971," in *Earthquakes in the USSR in 1971* (Nauka, Moscow, 1975) pp. 163–171.
19. N. A. Haskell, "Total Energy and Energy Spectral Density of Elastic Wave Radiation from Propagating Faults," *Bull. Seismol. Soc. Am.* **54**, 1811–1841 (1964).
20. N. A. Haskell, "Total Energy and Energy Spectral Density of Elastic Wave Radiation from Propagating Faults. II. A Stochastic Fault Model," *Bull. Seism. Soc. Am.* **56**, 125–140 (1966).
21. K. Irikura, "Lecture Note on Strong Motion Seismology," *Chapter 5. 8th Workshop 3D Modelling of Seismic Waves Generation, Propagation and their Inversion* (ICTP, Trieste, 2006).
22. Y. Izutani, "Source Parameters Relevant to Heterogeneity of a Fault Plane," *J. Phys. Earth.* **32**, 511–529 (1984).
23. J. Eioama, "Earthquake Source Time-Function from Coherent and Incoherent Rupture," *Tectonophysics* **118**, 227–242 (1985).
24. J. Eioama, M. Takemura, Z. Suzuki, "A Scaling Model for Quantification of Earthquakes in and near Japan," *Tectonophysics* **84**, 3–16 (1982).
25. A. S. Papageorgiou and K. Aki, "A Specific Barrier Model for the Quantitative Description of Inhomogeneous Faulting and the Prediction of the Strong Ground Motion. I. Description of the Model," *Bull. Seismol. Soc. Am.* **73**, 693–722 (1983).
26. A. S. Papageorgiou and K. Aki, "Scaling Law of Far-Field Spectra Based on Observed Parameters of the Specific Barrier Model," *Pure Appl. Geophys.* **123**, 354–374 (1985).

27. V. M. Pavlov, "A Convenient Technique for Calculating Synthetic Seismograms in a Layered Half-Space," *Proceedings Intern. Conf. Problems of Geocosmos* (St. Petersburg, 2002) pp. 320–323.
28. V. M. Pavlov, "Calculation of Static Displacements from the Force in the Layered Half-Space," *Vulkanologiya i Seismologiya*, No. 4, 25–33 (2006).
29. F. Schmitt and D. Marsan, "Stochastic Equations for Continuous Multiplicative Cascades in Turbulence," *Eur. Phys. J.* **20**, 3–6 (2001).
30. V. V. Shteinberg, V. M. Fremd, and V. D. Feofilaktov, "Ground Vibrations caused by the Strong Earthquakes in Kamchatka in 1971," *Strong Kamchatka Earthquakes of 1971* (Vladivostok, 1975) pp. 7–14.
31. V. M. Zobin, "The Process in the Source of Petropavlovsk Earthquake (on November 24, 1971)," *Vulkanologiya i Seismologiya*, No. 4, 91–103 (1984).
32. V. M. Zobin, S. A. Fedotov, E. I. Gordeev et al., "Strong Earthquakes in Kamchatka and Komandorskie Islands in 1961–1986," *Vulkanologiya i Seismologiya*, No. 1, 3–23 (1988).

SPELL: 1. @:,